

## Supporting Information

# Novel catalyst PTMA-PILC: structural properties and catalytic performance for the bioethanol dehydration to ethylene

Xianmei Xie\*<sup>a</sup>, Zheng Li<sup>a</sup>, Baoru Li<sup>a</sup>, Xu Wu<sup>a</sup>, Xia An<sup>a</sup>

## S1. Experimental

### 1.1 Catalyst characterization

The X-ray diffraction diagrams were recorded over powder sample on Rigaku D/max-2500 instrument (40 KV, 100 mA) using Cu K $\alpha$  radiation ( $\lambda = 0.154056$  nm) at a scanning speed of 0.13 °/s, with the scanning range of 4-35 °.

FT-IR spectra of the samples were performed on a Perkin-Elmer 1730 Infrared Fourier Transform Spectrometer between 400-4000 cm<sup>-1</sup> region. One milligram of sample and 300 mg of KBr were used in the preparation of the pellets.

The surface area and pore size distribution were determined from nitrogen adsorption-desorption isotherm data by the Brunauer-Emmett-Teller (BET) and Barret-Joyner-Halenda (BJH) methods using a Micro-meritics ASAP 2020 instrument. The isotherms were measured at 77 K using N<sub>2</sub>. Prior to determining the isotherms, the samples were degassed at 100 °C in vacuum ( $\approx 30$  Pa) for 70 min.

The temperature-programmed desorption of NH<sub>3</sub> (NH<sub>3</sub>-TPD) was carried out between 10 and 750 °C using Autochem II 2920 (Micromeritics Instruments). Prior to adsorption, the sample (0.04 g) was calcined under the N<sub>2</sub> flow of 50 mL/min at 300 °C for 1 h and then cooled to 50 °C. After that, it was treated by 10% NH<sub>3</sub>/He for 30 min. The nature and strength of acid sites were evaluated by IR spectroscopy of pyridine. For this analysis the sample was preheated at 300 °C for 2 h under vacuum pressure. Pyridine adsorption was run at room temperature during 30 min. Desorption was realised in vacuum at 150 °C and infrared spectra were recorded after thermal treatment.

Thermogravimetric analysis (TG) was performed on a NETZSCH-STA 409C thermobalance. Around 5 mg of sample at particle sizes of 100–200 mesh was used for each experimental and the heating temperature in the TG was in the range of 25–800 °C, and the heating rate was controlled at 10 °C/min. Nitrogen was used as the carrier gas in the TG which flow rate was fixed at 100 mL/min.

The microstructures of catalysts was investigated using transmission electron microscope (TEM, JEM-1011).

### 1.2 Catalytic performances test

The fixed-bed micro-reactor used for the catalytic performance tests is shown as Fig. 1 and the reaction of ethanol dehydration to ethylene was used to evaluate the catalytic behaviours of the solids. 1.0 g catalysts were dispersed in 3.0 g silica sand and loaded in the middle of a stainless steel reactor. The reactor was purged by nitrogen flow for 60 min, and the liquid reactant containing water and ethanol with the volume ratio of 7:3 was injected by a pulse micro-liquid pump into a vaporizer and subsequently passed into the reactor with the LHSV of 0.65 h<sup>-1</sup> with the operation temperature range from 200 to 600 °C. The temperatures of the vaporizer and the reactor were controlled by the thermocouples. Outlet products were condensed and separated by a gas-liquid separator. The gas concentrations were quantified on line by a haixin 950 gas chromatograph equipped with a FID and a TCD detector and two packed columns (GDX-401, TDX-01). The liquid products were analyzed off-line on another gas chromatograph equipped with a Porapak Q column. Ethanol conversion was denoted as C<sub>ethanol</sub> and S<sub>i</sub> represents the product distribution of i, they were calculated according to Eq. (S1) and (S2):

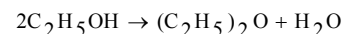
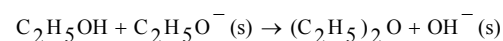
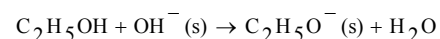
$$C_{\text{ethanol}} = \frac{n(\text{ethanol}_{\text{in}}) - n(\text{ethanol}_{\text{out}})}{n(\text{ethanol}_{\text{in}})} \times 100\% \quad (\text{S1})$$

$$S_i = \frac{n(P_i)}{\sum_{i=1}^n n(P_i)} \times 100\% \quad (\text{S2})$$

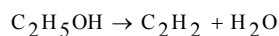
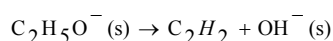
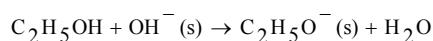
## S2. Reaction mechanism of ethanol dehydration

On OH<sup>-</sup> rich metal oxide surfaces, the following pathways have been proposed<sup>S1</sup>:

1. Diethyl ether formation:

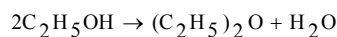
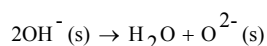
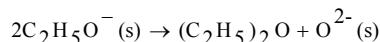
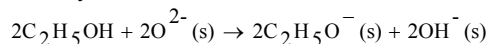


2. Ethene formation:



On OH- poor surfaces, the following mechanisms have been suggested<sup>S1</sup>:

1 Diethyl ether formation:



2. Ethene formation:

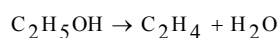
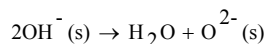
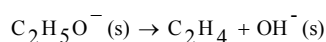
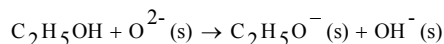


Table S1. The compositions of Na-MMT

Sample (wt%)	Al <sub>2</sub> O <sub>3</sub>	CaO	Fe <sub>2</sub> O <sub>3</sub>	K <sub>2</sub> O	MgO	Na <sub>2</sub> O	P <sub>2</sub> O <sub>5</sub>	SO <sub>3</sub>	TiO <sub>2</sub>	SiO <sub>2</sub>	Loss on ignition
Na-MMT	19.55	2.58	1.71	0.68	3.63	4.06	0.08	0.07	0.06	61.18	6.4

Table S2. Textural characteristics of different catalysts

Catalyst	BET surface area (m <sup>2</sup> /g)	Pore Size/nm	SiO <sub>2</sub> (wt%) <sup>a</sup>	Al <sub>2</sub> O <sub>3</sub> (wt%) <sup>a</sup>	P <sub>2</sub> O <sub>5</sub> (wt%) <sup>a</sup>	MoO <sub>3</sub> (wt%) <sup>a</sup>
Na-MMT	21	3.7	61.18	19.55	0.08	--
AT-MMT	335	9.1	77.49	9.85	--	--
PILC	301	3.7	70.49	14.99	--	--
PTMA-	253	3.4	65.27	15.92	0.227	2.383

<sup>a</sup>The content of SiO<sub>2</sub>, Al<sub>2</sub>O<sub>3</sub>, P<sub>2</sub>O<sub>5</sub> and MoO<sub>3</sub> over the montmorillonites was determined by XRF.

Table S3. The acid distributions on different catalysts.

Catalysts	Temperature	Weak acid amount (mmol/g)
Na-MMT	90	0.086
AT-MMT	90	0.112
PICL	90	0.175
PTMA-PILC	93	0.178

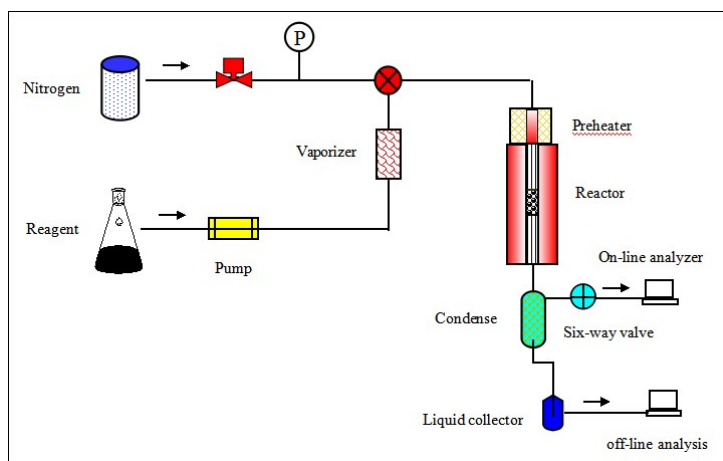


Fig. S1. Reaction equipment for the Ethanol dehydration to ethylene

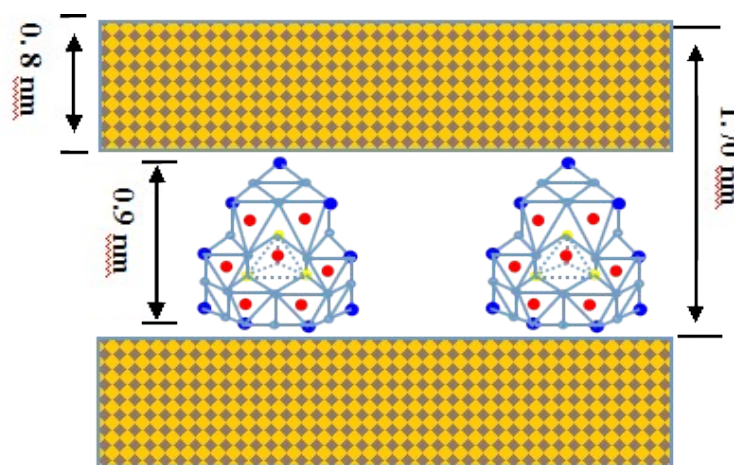
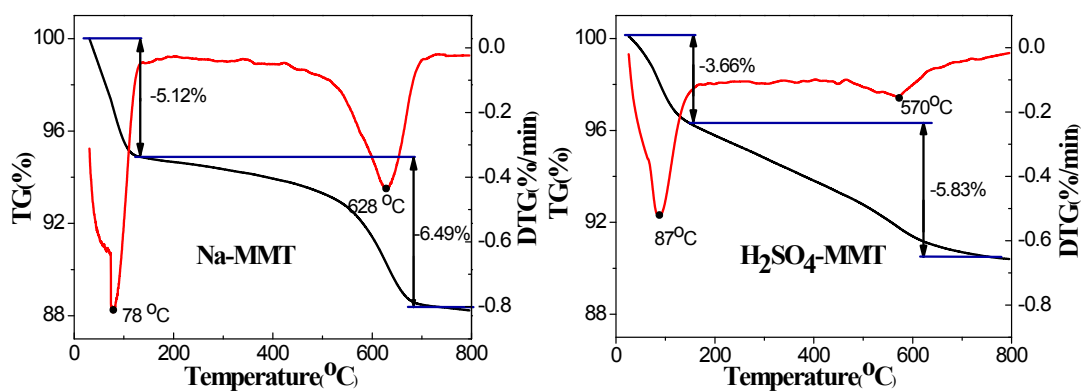


Fig. S2. Schematic diagram of Al<sub>13</sub><sup>7+</sup> in the midst of structure unit layer of PILC (a)



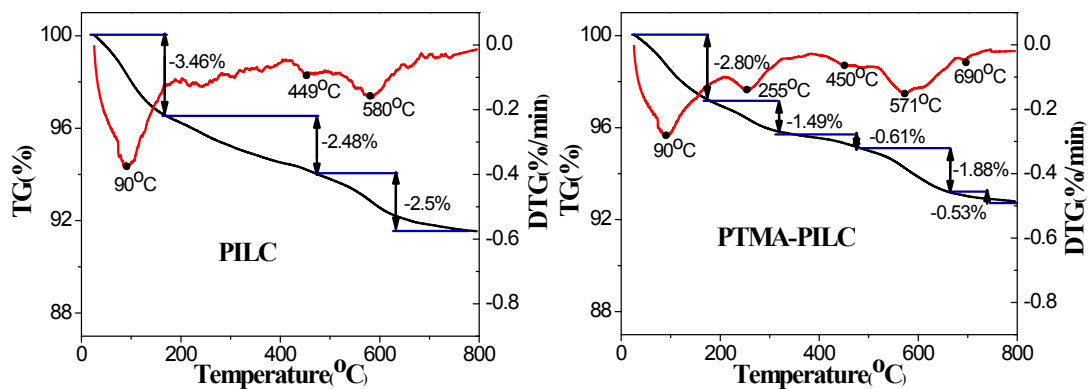


Fig. S3. TG and DTG of different catalysts

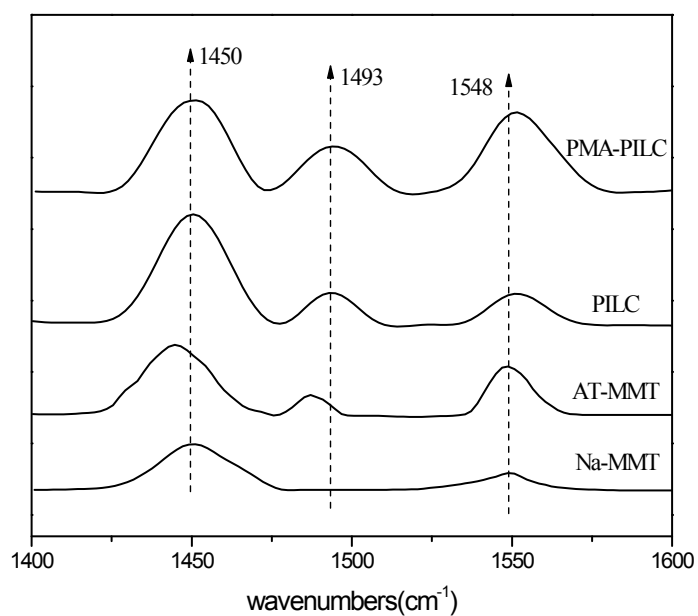


Fig. S4. IR spectra of pyridine adsorbed on different catalysts

### S3 References

S1. S. Golay, L. Kiwi-Minsker, R. Doepper and A. Renken, *Chem Eng Sci.* 1999, **54**, 3593-3598.